Journal of Medicinal Chemistry

Article

pubs.acs.org/jmc

New 2-(Aryloxy)-3-phenylpropanoic Acids as Peroxisome Proliferator-Activated Receptor α/γ Dual Agonists Able To Upregulate Mitochondrial Carnitine Shuttle System Gene Expression

A. Laghezza,[†] G. Pochetti,[§] A. Lavecchia,[∥] G. Fracchiolla,[†] S. Faliti,[†] L. Piemontese,[†] C. Di Giovanni,[∥] V. Iacobazzi,[‡,⊥] V. Infantino,[‡,#] R. Montanari,[§] D. Capelli,[§] P. Tortorella,[†] and F. Loiodice*[,†]

[†]Dipartimento di Farmacia-Scienze del Farmaco and [‡]Laboratorio di Biochimica e Biologia Molecolare, Dipartimento di Bioscienze, Biotecnologie e Biofarmaceutica, Università degli Studi di Bari "Aldo Moro", 70126 Bari, Italy

[§]Istituto di Cristallografia, Consiglio Nazionale delle Ricerche, Montelibretti, 00015 Monterotondo Stazione, Roma, Italy

[∥]Dipartimento di Chimica Farmaceutica e Tossicologica, Università di Napoli "Federico II", 80131 Napoli, Italy

[⊥]Istituto di Biomembrane e Bioenergetica, Consiglio Nazionale delle Ricerche, 70126 Bari, Italy

[#]Dipartimento di Chimica, Università della Basilicata, 85100 Potenza, Italy

Supporting Information

ABSTRACT: The preparation of a series of 2-(aryloxy)-3-phenylpropanoic acids, resulting from the introduction of different substituents into the biphenyl system of the previously reported peroxisome proliferator-activated receptor α/γ (PPARα/γ) dual agonist **1**, allowed the identification of new ligands with higher potency on PPARα and fine-tuned moderate PPARγ activity. For the most promising stereoisomer (*S*)-**16**, X-ray and calorimetric studies in PPARγ revealed, at high ligand concentration, the presence of two molecules simultaneously bound to the receptor. On the basis of these results and docking experiments in both receptor subtypes, a molecular explanation was provided for its different behavior as a full and partial agonist of PPARα and PPARγ, respectively. The effects of (*S*)-**16** on mitochondrial acylcarnitine carrier and carnitine-palmitoyl-transferase 1 gene expression, two key components of the carnitine shuttle system, were also investigated, allowing the hypothesis of a more beneficial pharmacological profile of this compound compared to the less potent PPARα agonist fibrates currently used in therapy.

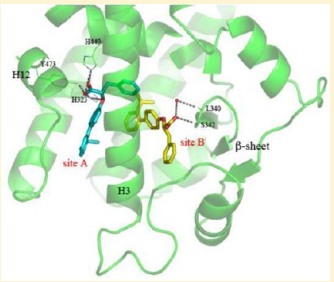

INTRODUCTION

Peroxisome proliferator-activated receptors (PPARs) are ligand-activated transcription factors belonging to the nuclear hormone receptor superfamily. They are lipid sensors activated by specific ligands, which are usually lipophilic small molecules.[1] Binding of these ligands results in conformational changes of the receptors that facilitate their interaction with coactivator proteins in the nucleus.[2−4] The resulting protein complexes activate the transcription of specific target genes, resulting in the induction of intracellular signaling cascades that mediate the physiological effects of the ligands.[5,6]

There are three distinct subtypes, PPARα, PPARγ, and PPARδ, which are encoded by different genes. The different PPARs have different tissue distributions and modulate different physiological functions. PPARs play a key role in various aspects of the regulation of a large number of genes; the products of these genes are directly or indirectly involved in energy homeostasis and lipid and carbohydrate metabolism. The fibrate class of lipid-lowering drugs (e.g., fenofibrate and gemfibrozil) are PPARα ligands.[7,8] The marketed thiazolidinedione (TZD) class of antidiabetic agents (rosiglitazone and pioglitazone) activate PPARγ.[9] They enhance insulin sensitivity in target tissues and lower glucose and fatty acid levels in type 2 diabetic patients. The success of the hypolipidemic fibrates and TZD class of insulin sensitizers has prompted pharmaceutical companies to concentrate on developing more potent and dual agonists acting on these two subtypes. Dual-acting PPARα/γ agonists, in fact, are considered a very attractive option in the treatment of dyslipidemic type 2 diabetes.[10−18]

One of the key challenges for the development of a dual agonist is the identification of the optimal receptor subtype selectivity ratio. PPARγ full agonists, in fact, despite their proven benefits, have been plagued by certain adverse effects such as weight gain, higher rate of bone fractures, fluid accumulation, and pulmonary edema, leading to increased frequency of congestive heart failure.[19−21] However, as demonstrated from the problems that many dual agonists have encountered during their development, an ideal PPARα/γ activity ratio probably does not exist. For a specific series of strictly related ligands, in fact, this value depends on many factors such as tissue selectivity and ability to recruit particular coactivator proteins and activate the transcription of specific target genes. During the past decade, therefore, new drugs

Received: July 12, 2012
Published: November 22, 2012

Table 1. Activity of the Tested Compounds in Cell-Based Transactivation Assay

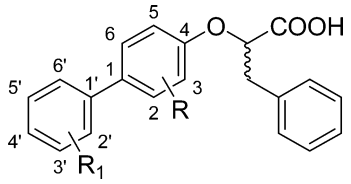

				PPARα		PPARγ	
compd	config	R	R_1	EC_{50} (μM)	E_{max}[a]	EC_{50} (μM)	E_{max}[a]
1	*S*	H	H	0.19 ± 0.04	116 ± 4	0.55 ± 0.12	62 ± 7
2	*S*	3-CH_3	H	0.99 ± 0.08	68 ± 8	0.70 ± 0.10	34 ± 4
3	*S*	2-CH_3	H	0.08 ± 0.03	120 ± 9	0.70 ± 0.04	47 ± 3
4	*S*	3,5-$(CH_3)_2$	H	1.13 ± 0.03	61 ± 1	3.1 ± 0.6	18 ± 1
5	*R*,*S*	2,6-$(CH_3)_2$	H	2.1 ± 0.5	50 ± 16	2.04 ± 1.10	13 ± 1
6	*S*	H	2′,6′-$(CH_3)_2$	0.23 ± 0.04	123 ± 13	2.54 ± 0.37	16 ± 1
7	*S*	H	4′-CH_3	0.21 ± 0.09	74 ± 3	0.59 ± 0.26	47 ± 1
8	*R*,*S*	H	3′-CH_3	0.22 ± 0.08	69 ± 4	0.46 ± 0.13	43 ± 4
9	*S*	H	2′-CH_3	0.067 ± 0.005	155 ± 12	1.36 ± 0.26	42 ± 4
10	*S*	2-CH_3	2′-CH_3	0.031 ± 0.002	133 ± 8	0.64 ± 0.14	49 ± 2
11	*S*	H	2′-F	0.12 ± 0.04	68 ± 6	0.69 ± 0.19	37 ± 6
12	*S*	H	2′-CF_3	0.022 ± 0.002	126 ± 6	1.00 ± 0.14	32 ± 2
13	*S*	H	2′-Ph	0.044 ± 0.028	132 ± 5	1.4 ± 0.7	10 ± 1
14	*S*	H	2′-OCH_3	0.13 ± 0.06	124 ± 14	2.30 ± 0.01	21 ± 6
15	*S*	H	2′-C_2H_5	0.012 ± 0.002	143 ± 8	1.2 ± 0.4	28 ± 2
(*S*)-**16**	*S*	H	2′-*i*Pr	0.012 ± 0.007	147 ± 20	1.0 ± 0.2	33 ± 3
(*R*)-**16**	*R*	H	2′-*i*Pr	0.10 ± 0.03	145 ± 24	nc	12 ± 8
17	*R*,*S*	H	2′-*n*Pr	0.24 ± 0.01	131 ± 4	nc	8 ± 6
18	*R*,*S*	H	2′-nC_5H_{11}	0.50 ± 0.05	107 ± 20	nc	11 ± 6
19	*R*,*S*	H	2′-CH_2CH_2Ph	0.28 ± 0.03	73 ± 11	nc	7 ± 2
Wy 14,643				1.56 ± 0.30	100 ± 10	ia	ia
rosiglitazone				ia	ia	0.039 ± 0.003	100 ± 9

[a]Efficacy values were calculated as a percentage of the maximum obtained fold induction with the reference compounds. ia = inactive at tested concentrations (up to 10 μM). nc = not computable; the activity, in fact, increases with increasing concentrations up to 10 μM, above which the activity begins to decrease.

acting as full agonists of PPARα and partial agonists of PPARγ have been developed with the goal of retaining the beneficial effects while reducing the adverse effects.

Recently, we reported the synthesis and activity of the new ligand **1** (Table 1), which is a dual PPARα/γ ligand with a partial agonism profile toward the γ subtype.[22] The X-ray structure of the complex with PPARγ shows that this ligand occupies a branch, named the "biphenyl pocket", of a new L-shaped region of the PPARγ ligand binding domain (LBD) never sampled before by other known ligands and increases the stabilization of the helix H3, inducing a conformation of the LBD less favorable to the recruitment of coactivators required for full activation of PPARγ.[22] As regards PPARα, the ligand assumes a different orientation in the LBD that better stabilizes the helices H11 and H12, resulting in a full agonism response. The identification of these novel ligand−receptor interaction modalities represents a new hallmark of the partial agonism behavior of certain ligands and could be exploited for the design of new antidiabetic agents appropriately targeting the PPARs. Since **1** occupies only the first branch of the new L-shaped region, we decided to prepare some analogues characterized by the presence of a substituent, with different lengths and stereoelectronic properties, on the aromatic rings of the biphenyl system that could allow the complete occupation of the entire cavity and the evaluation of the effects due to a further stabilization of H11, H12, and the loop 11/12. The aim was the identification of a series of ligands which, while maintaining high potency and efficacy on PPARα, presented a fine-tuned moderate PPARγ activity. This could allow investigation, in a series of strictly related compounds, of the effects due to small differences in PPARγ activity and identification of the optimal selectivity ratio for this series of dual agonists. For this purpose, we synthesized the new 2-(aryloxy)-3-phenylpropanoic acids **2**−**19** reported in Table 1 and evaluated their PPARα/γ activity. Considering the high degree of stereoselectivity displayed from these receptors toward the stereoisomer **1**,[22] most derivatives were synthesized only as the *S* isomers. Noteworthy, we identified new ligands showing full agonism and higher potency on PPARα while maintaining basically unchanged potency on PPARγ with efficacy variable in the 10−50% range. For compound (*S*)-**16**, X-ray and calorimetric studies with PPARγ and docking experiments with both receptor subtypes were performed to provide a molecular explanation for its different activity. This ligand was selected because it was the most potent PPARα full agonist with fairly good potency and concomitant moderate efficacy on PPARγ (about 3-fold less effective than rosiglitazone). Finally, we investigated the effects of (*S*)-**16** on mitochondrial carnitine/acylcarnitine carrier (CAC) and carnitine-palmitoyl-transferase 1 (CPT1) gene expression. These two molecular components of the carnitine shuttle system are essential for the mitochondrial oxidation of fatty

dx.doi.org/10.1021/jm301018z | J. Med. Chem. 2013, 56, 60−72

Scheme 1. Synthesis of PPAR Agonists 2−16[a]

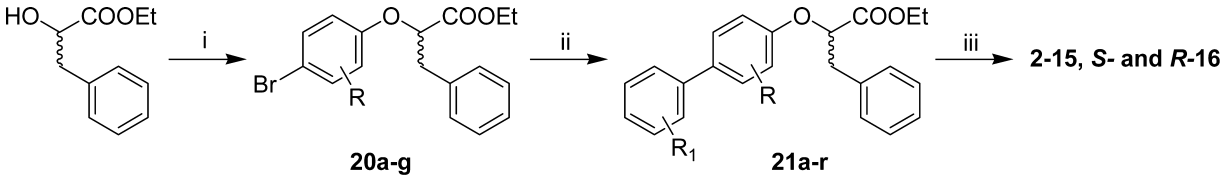

Compounds 20a-g	Compounds 21a-r	
a. R = H; (*S*)	**a.** R = 3-CH_3; R_1 = H	**b.** R = 2-CH_3; R_1 = H
b. R = H; (*R*)	**c.** R = 3,5-$(CH_3)_2$; R_1 = H	**d.** R = 2,6-$(CH_3)_2$; R_1 = H
c. R = H; (*R,S*)	**e.** R = H; R_1 = 2',6'-$(CH_3)_2$	**f.** R = H; R_1 = 4'-CH_3
d. R = 2-CH_3	**g.** R = H; R_1 = 3'-CH_3	**h.** R = H; R_1 = 2'-CH_3
e. R = 3-CH_3	**i.** R = 2-CH_3; R_1 = 2'-CH_3	**l.** R = H; R_1 = 2'-F
f. R = 2,6-$(CH_3)_2$	**m.** R = H; R_1 = 2'-CF_3	**n.** R = H; R_1 = 2'-Ph
g. R = 3,5-$(CH_3)_2$	**o.** R = H; R_1 = 2'-OCH_3	**p.** R = H; R_1 = 2'-CH_3CH_2
	q. R = H; R_1 = 2'-*i*-Pr; (*S*)	**r.** R = H; R_1 = 2'-*i*-Pr; (*R*)

[a]Reagents and conditions: (i) ArOH, DVB−PPh_3, DIAD, dry toluene; (ii) $ArB(OH)_2$, Cs_2CO_3, DVB−$Pd(PPh_3)_4$ or $Pd(PPh_3)_4$, dry toluene, reflux; (iii) 1 N NaOH, THF, rt.

acids because they catalyze the entry of fatty acid acyl groups into the mitochondrial matrix where the enzymes of fatty acid *β*-oxidation are located. Recent studies demonstrated that the transcription of the CAC gene is enhanced by statins and fibrates, providing, therefore, a novel contribution to the understanding of their hypolipidemic action.[23−25]

CHEMISTRY

The synthesis of compounds **2−16** is depicted in Scheme 1 and was carried out starting from the ethyl ester of racemic phenyllactic acid or (*R*)-phenyllactic acid and the suitably substituted 4-bromophenol, which were condensed, under Mitsunobu conditions, to obtain the key intermediates **20a−g**.[22] These underwent Suzuki coupling by condensation with the suitable boronic acids to give esters **21a−r**, which were hydrolyzed to the desired acids. Through this procedure acid (*R*)-**16** was prepared as well; in this case (*S*)-ethyl phenyllactate was used as the starting material. Alternatively, to reduce the unacceptably long reaction time required for the Suzuki coupling under normal conditions, the appropriate intermediate **20c** was condensed with 2-formylphenylboronic acid in a microwave reactor to give compound **22** (Scheme 2). Wittig reaction of **22** with the suitable substrates afforded the unsaturated intermediates **23a−c**, which were reduced under hydrogen pressure in the presence of the Wilkinson catalyst or 10% palladium on carbon to give esters **24a−c**, whose alkaline hydrolysis led to the target acids **17−19**. The attempt to obtain, by this procedure, the *S* isomers of **17−19** starting from **20a** failed due to the racemization process occurring in the Wittig reaction.

Scheme 2. Synthesis of PPAR Agonists 17−19[a]

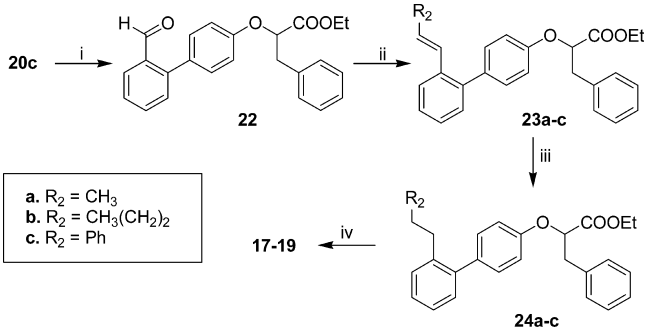

[a]Reagents and conditions: (i) 2-formylphenylboronic acid, Cs_2CO_3, $Pd(PPh_3)_4$, THF; microwave, 100 °C, 150 W, 1 h; (ii) $R_2CH_2P(Ph)_3X$, DBU, dry CH_3CN, N_2, reflux; (iii) H_2 (10−15 atm), Wilkinson catalyst, EtOH, rt for esters **24a,b** or 10%Pd/C, EtOH, rt for ester **24c**; (iv) 1 N NaOH, THF, rt.

The enantiomeric excess (ee) of all optically active isomers was determined by HPLC on a chiral stationary phase (see the Experimental Section). For this purpose, small amounts of the corresponding racemates were also prepared starting from racemic ethyl phenyllactate. In most cases, the ee was higher than 94−95%; only acids **10**, **11**, **12**, and **14** showed an ee in the 75−88% range.

RESULTS AND DISCUSSION

Compounds **2−19** were evaluated for their agonist activity on the human PPAR*α* (hPPAR*α*) and PPAR*γ* (hPPAR*γ*) subtypes. For this purpose, GAL4-PPAR chimeric receptors were expressed in transiently transfected HepG2 cells according to a previously reported procedure.[26] The results obtained (Table 1) were compared with corresponding data for Wy-14,643 and rosiglitazone used as reference compounds in the PPAR*α* and PPAR*γ* transactivation assays, respectively. The maximum induction obtained with the reference agonist was defined as 100%.

We first set the series of derivatives **2−10** bearing one or two methyl groups on different positions of the biphenyl system with the aim to identify the most promising sites of substitution in terms of potency and efficacy. As shown in Table 1, when at least a methyl group was located ortho to the biphenyl simple bond, full agonists of PPAR*α* were obtained with similar (**6**) or 2−6-fold higher (**3**, **9**, **10**) potency as compared to lead compound **1**. It is reasonable to hypothesize that the presence of a methyl in this position induces the biphenyl system of these ligands to assume a torsion angle favoring interactions with the receptor. The only exception was represented from the 2,6-dimethyl derivative **5** exhibiting relatively low potency and partial agonism; even though this compound was tested as a racemate, in fact, it must be taken into account that its possible

dx.doi.org/10.1021/jm301018z | J. Med. Chem. 2013, 56, 60−72

S eutomer would have at most a 2-fold higher potency than the racemate with unchanged efficacy. In this case, it is likely that the concomitant presence of two methyls in these positions of the proximal benzene ring causes some steric clash, which does not allow a favorable accommodation of the molecule into the binding site. The introduction of a methyl in other positions of the biphenyl nucleus still afforded potent PPARα activators (**2**, **4**, **7**, **8**) endowed, however, with partial agonist activity. As regards PPARγ activity, derivatives **2**−**10** were all partial agonists with lower potency compared to PPARα. No correlation was found between activity and the type of substitution, suggesting less constraining structural requirements for these ligands in PPARγ. These analogues showed the desired variability of efficacy, which ranged from 15% to 50%; however, with the aim to search for even more potent PPARα agonists, we decided on an in-depth investigation of the ortho position to the biphenyl bond, which seemed to be the most promising site to achieve this result. For this reason, we decided to synthesize compounds **11**−**19** in which the methyl group located in the 2′ site of **9** was replaced by substituents with different stereoelectronic properties. Most derivatives exhibited full agonism toward PPARα with submicromolar potency. The activity was increased about 5-fold by replacing the methyl with ethyl (**15**) or a branched alkyl group such as isopropyl (**16**), whereas it remained almost unchanged with the introduction of an *n*-propyl (**17**); this last compound, however, was tested as a racemate as well as **18**, in which a further lengthening of the alkyl chain to pentyl afforded a marked reduction of activity probably due to the lack of steric requirements. More potent agonists were also achieved by increasing lipophilicity as shown from trifluoromethyl and phenyl derivatives **12** and **13**, respectively. When the benzene ring of **13** was moved away from biphenyl by introduction of an ethyl chain (**19**), a 6-fold decrease in potency resulted, suggesting a possible reduced capacity to form a favorable $\pi-\pi$ interaction with some residues of the receptor and/or a poor accommodation of the phenethyl group into the binding pocket because of its steric hindrance. Also in this case, however, it must be taken into account that **19** was tested as a racemate. PPARα activity, on the contrary, seemed to be less affected by the electronic properties of the substituents; the presence of an electron-withdrawing fluorine (**11**) or an electron-releasing methoxyl (**14**) afforded, in fact, ligands with the same potency even though they had different efficacies. It is possible that, in this set of analogues, the right size of the substituent is needed to obtain the best PPARα activity: too small or too large substituents, in fact, seem to not be appropriate for a favorable interaction with the receptor. As regards PPARγ, also in this case, all derivatives **11**−**19** displayed lower potency and efficacy compared to PPARα. No relevant difference of activity was observed by changing the electronic and lipophilic properties of the substituents with the exception of methoxyl derivative **14**, which, differently from PPARα, was 3 times less potent than fluoro derivative **11**. Steric requirements, also, did not significantly affect activity as shown from the similar potency and efficacy of **9**, **15**, and **16**. However, compounds **17**−**19** with long-chain substituents exhibited poor activity up to 5−10 μM, suggesting that spatial limitation may exist for the binding pocket that accommodates this part of the molecule.

At this point, with the aim to confirm the importance of stereochemistry in PPAR activation, we decided to prepare the *R* configurational isomer of the isopropyl derivative **16**. The preference went to this compound because it apparently showed the best dual agonist profile on the α and γ subtypes. It was, in fact, the most potent PPARα full agonist with fairly good potency and concomitant moderate efficacy on PPARγ (about 3-fold less effective than rosiglitazone). Actually, this stereoisomer displayed a singular behavior; it was almost inactive on PPARγ and about 10 times less potent than the corresponding *S* isomer on PPARα. However, it behaved as a full agonist toward PPARα, showing equipotency with lead compound **1** and higher potency than reference compound Wy-14,643, allowing the hypothesis that the presence of a substituent with appropriate stereoelectronic properties placed ortho to the biphenyl bond of the ligand is able to counterbalance the lack of a correct spatial arrangement of the groups bound to the stereogenic center.

With the aim to provide a molecular explanation for the different behavior of (*R*)- and (*S*)-**16** compared to **1**, X-ray crystal studies in PPARγ-LBD have been performed for both enantiomers.

Binding of (*S*)-16 in the PPARγ-LBD. The final simulated annealing omit map (Figure 1 of the Supporting Information) clearly shows two molecules of (*S*)-**16** simultaneously bound to PPARγ-LBD. One molecule (mol A) is accommodated into the biphenyl pocket (site A), as its analogue **1** lacking the isopropyl group,[22] and interacts with the triad H323, H449, and Y473. The second molecule (mol B) binds in the typical position of the pure partial agonists of PPARγ,[22,27] facing the β-sheet and interacting with it through H-bonds (site B). Moreover, the two molecules interact with each other, making short van der Waals (vdW) contacts through the isopropyl group of mol B and the benzylic aromatic ring of mol A (Figure 1). The presence of

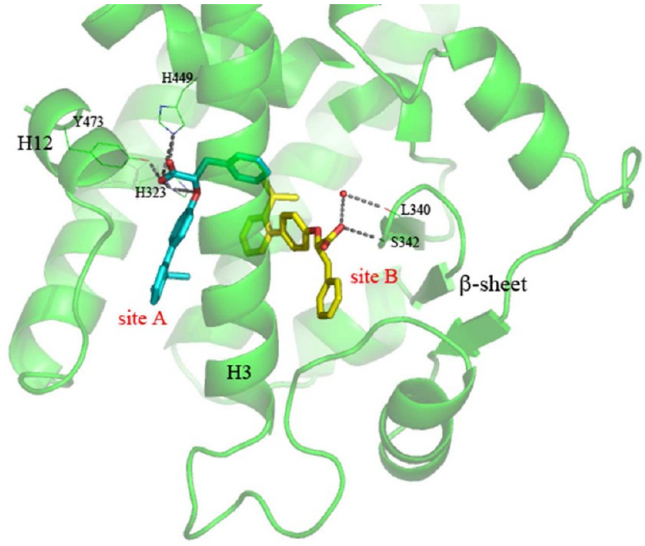

Figure 1. (*S*)-**16** in the complex with PPARγ: mol A (cyan) positioned into the biphenyl pocket and mol B (yellow) in front of the β-sheet.

two molecules of the ligand is also confirmed by indirect evidence; in fact, the side chains of R288 and E291 are dramatically rearranged for the presence of the ligand in site B, and the side chain of F282 is shifted from the *t* to the folded *g** conformation for the presence of a second molecule in site A. However, the weak electron density on the side chain of F282 denotes a probable disorder of this residue on site A. This could be attributed to the steric hindrance of the bulky isopropyl-substituted biphenyl moiety into the narrow biphenyl pocket. This is also confirmed by the weak electron density on the

dx.doi.org/10.1021/jm301018z | J. Med. Chem. 2013, 56, 60−72

isopropyl group that interacts with very short vdW contacts with the side chain of F282.

On site B, the carboxylate oxygens of mol B form H-bonds with the NH of S342 and CO of L340 on the β-sheet, the last one mediated by a water molecule. Moreover, several vdW contacts are formed by mol B with the side chains of F264, C285, M364, and L330 (Figure 2).

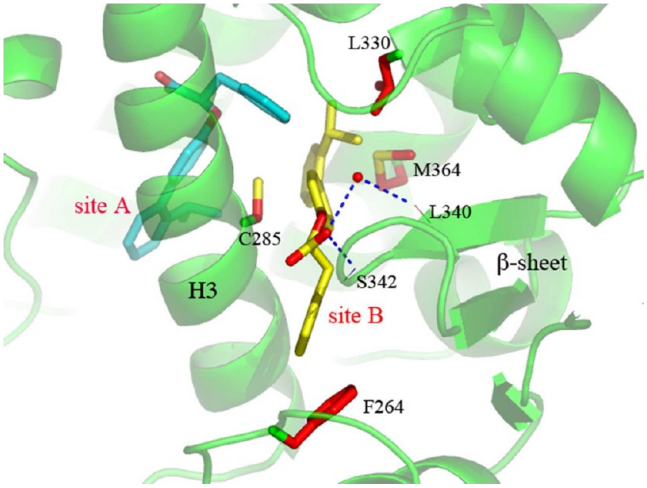

Figure 2. H-bond network and vdW interactions of mol B of (*S*)-**16** (yellow) in site B of PPARγ-LBD.

Binding of (*R*)-16 in the PPARγ-LBD. In this case the occupation of the only site B is observed. Unlike mol B of its *S* enantiomer, (*R*)-**16** is shifted more toward the entrance of the LBD (Figure 2 of the Supporting Information). Site A is empty as confirmed also by the clear density on the F282 side chain in the *trans* conformation to close the entrance to the biphenyl pocket. One water molecule coordinates the triad H323, H449, and Y473. Also in this case R288 and E291 side chains are dramatically rearranged to allow the occupation of site B by the ligand. The carboxylate group forms H-bonds with the NH of S342, and the benzylic aromatic ring of the ligand is sandwiched between those of F287 and H266, giving rise to strong vdW interactions (Figure 3).

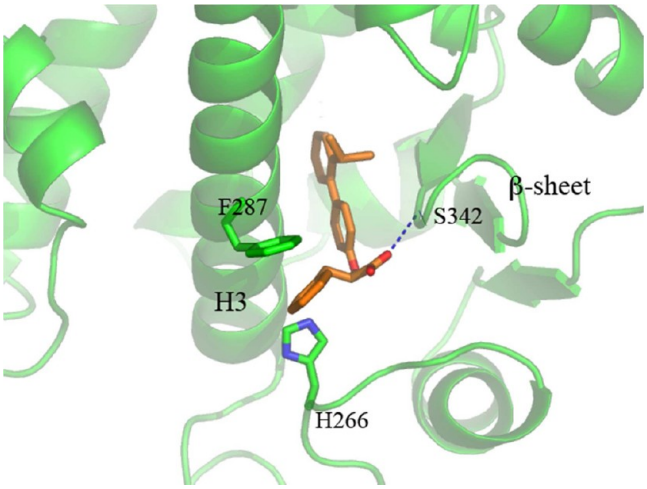

Figure 3. H-bond network and vdW interactions of (*R*)-**16** in the LBD of PPARγ.

Calorimetric Measurements. With the aim to evaluate the binding characteristics of (*S*)-**16** and those of the corresponding enantiomer (*R*)-**16**, we decided to perform isothermal titration calorimetry (ITC) experiments. This analysis directly gives the standard enthalpy change ΔH associated with the formation of the receptor−ligand complex, the estimation of ΔG, and the host−guest stoichiometry (n) by titration curve fitting. The entropy change ΔS can also be calculated from the Gibbs−Helmholtz equation. The ITC measurements were carried out at 298 K in 20 mM Hepes buffer at pH 8. Figure 4a shows the calorimetric data (raw and integration data) obtained in the titration of PPARγ with (*S*)-**16**. The same experiment was also conducted for **1** and (*R*)-**16** (Figures 3 and 4 of the Supporting Information, respectively). After subtraction of the heat of dilution from the raw data and linear curve fitting under the "one set of sites model", the thermodynamic parameters shown in Table 2 were obtained. For (*S*)-**16** the inflection point in the calorimetric isotherm occurs near the molar ratio of 1.0, which corresponds to a 1:1 binding mode ($K_a = 3.60 \times 10^5$ M^{-1}). To check if the ligand had multiple binding sites, as found in the X-ray experiments, a reverse titration was performed in which a 400 μM solution of protein was injected into the cell containing a diluted solution of the ligand (40 μM). For 1:1 bimolecular reactions, the measured thermodynamic parameters are expected to remain unchanged when the experiment is conducted in reverse order. On the contrary, the reverse titration (shown in Figure 4b) has the inflection point near the molar ratio of 0.5 (i.e., two molecules of ligand for one of protein), indicating that when the ligand is in large excess (10:1 ratio at the beginning of the experiment), the prevailing binding mode is 2:1. To establish the affinity of (*S*)-**16** toward each site, a third experiment was performed in which the protein was pre-equilibrated in a 1:1 ratio with lead compound **1**, which occupies only site A, as observed in the crystal structure of the complex PPARγ/**1**.[22] After pre-equilibration, the protein (47 μM) was titrated with (*S*)-**16** (470 μM) (Figure 4c). Given the higher affinity for site A of **1** with respect to (*S*)-**16**, ($K_a = 4.59 \times 10^5$ M^{-1} vs 3.60×10^5 M^{-1}, respectively), (*S*)-**16** should not be able to displace **1** from site A, unless it is in large excess. Thus, in this case, binding could be mainly referred to the second binding site (site B). As expected, the titration gave a lower affinity constant ($K_a = 1.87 \times 10^5$ M^{-1}) and a stoichiometry of 0.7.

The analysis of these ITC experiments shows that, at ligand/protein ratios not higher than 2:1 (final conditions of the experiment shown in Figure 4a), (*S*)-**16** binds to the higher affinity binding site ($K_a = 3.60 \times 10^5$ M^{-1}); a similar affinity was measured for the binding of lead compound **1** in the biphenyl pocket (site A, $K_a = 4.59 \times 10^5$ M^{-1}) (Figure 3 of the Supporting Information). The similarity between these K_a values seems to confirm that site A is the one with the higher affinity. When the protein is pre-equilibrated with **1** in a 1:1 ratio, site A is already occupied and the titration with (*S*)-**16** leads new molecules to preferentially bind to the available site B, resulting in a protein with both sites occupied, although site B seems to be engaged only at 70% ($n = 0.70$). In this case the titration affords the K_a (1.87×10^5 M^{-1}) and the other thermodynamic parameters for site B (Table 2). This K_a value is close to that obtained by titrating (*R*)-**16** (1.34×10^5 M^{-1}; see below), corresponding to the occupation of the only site B. This similarity indirectly confirms that this K_a value is an effective measure of (*S*)-**16** for site B.

dx.doi.org/10.1021/jm301018z | *J. Med. Chem.* 2013, 56, 60−72

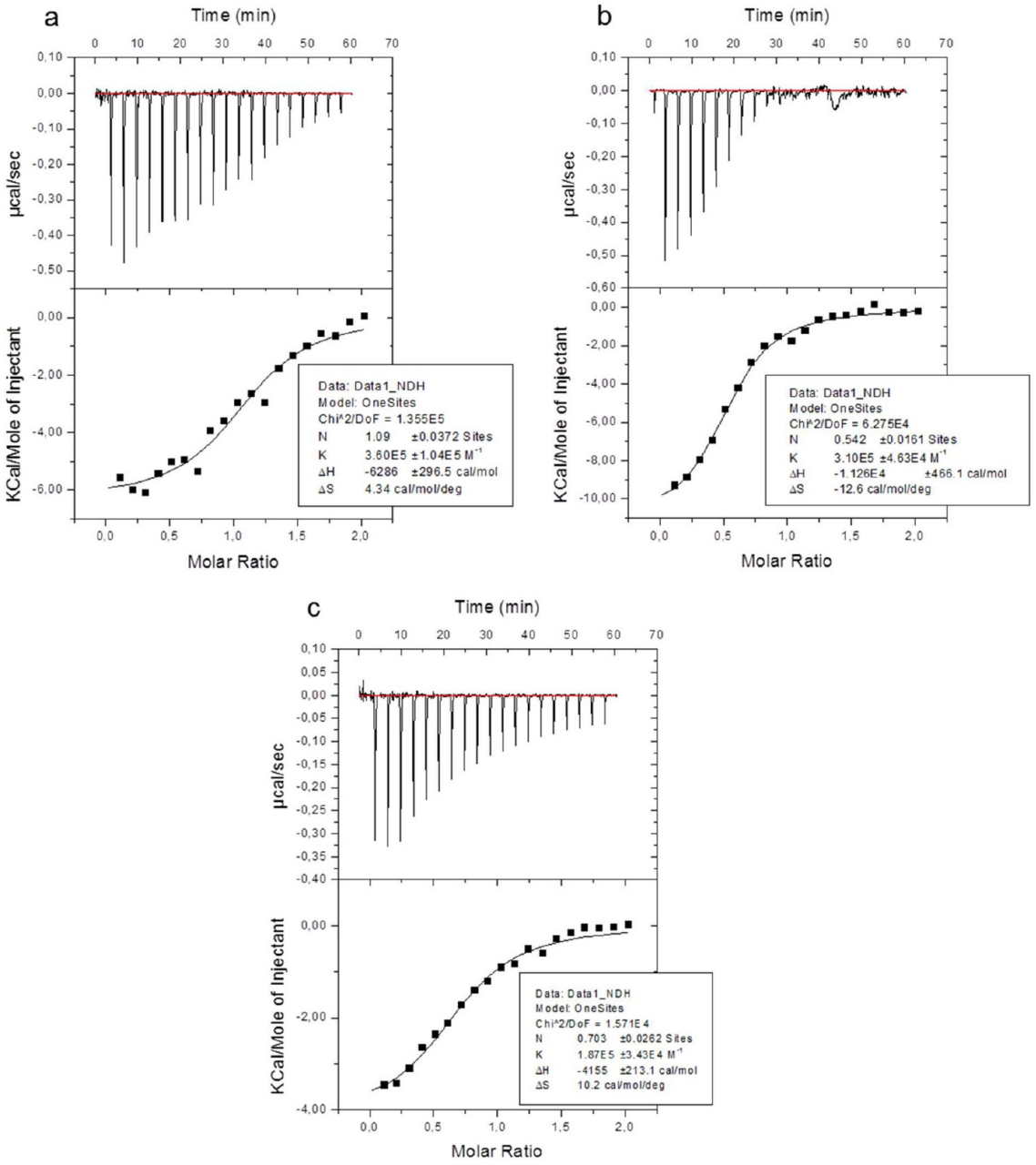

Figure 4. (a) Titration of PPARγ (40 μM) with (*S*)-**16** (400 μM). (b) Reverse titration of (*S*)-**16** (40 μM) with PPARγ (400 μM). (c) Titration with (*S*)-**16** (470 μM) of PPARγ (47 μM) after pre-equilibration with **1** (ratio 1:1).

As noted in Table 2, the enthalpy change in the reverse titration (site A + site B, ΔH = −11.26 kcal/mol) approximately corresponds to the sum of ΔH values measured for the single occupation of site A and site B (−6.29 and −4.15 kcal/mol, respectively) plus an additional amount probably due to the direct interaction of the two molecules in the LBD. The K_a value measured in this experiment (3.10×10^5 M^{-1}) is within those calculated for each site (3.60×10^5 and 1.87×10^5 M^{-1}). Despite the favorable enthalpic contribution due to the binding of two molecules (ΔH = −11.26 kcal/mol), a very unfavorable entropic term ($-T\Delta S$ = 3.79 kcal/mol) leads the net free energy to a value slightly lower than that of the binding on site A (−7.47 vs −7.58 kcal/mol, respectively). This could suggest a conformational rearrangement of the protein upon the binding of two molecules, which may act as an energy barrier.

The ITC titration of the ligand (*R*)-**16** (600 μM) into the cell containing PPARγ (60 μM) is shown in Figure 4 of the Supporting Information. The binding mode of the ligand is 1:1 (n = 0.99), and the K_a corresponding to the occupation of site B is 1.34×10^5 M^{-1}. The reverse titration performed for (*R*)-**16** (Figure 5 of the Supporting Information) shows a stoichiometry n value of 0.44, indicating also for this ligand a 2:1 binding mode with both sites of similar affinity. The K_a value of 1.30×10^5 M^{-1} obtained from this experiment is almost identical to that of site B ($K_a = 1.34 \times 10^5$ M^{-1}), suggesting the existence of a second low-affinity site (site C), which, however, was not observed in the crystal complex of PPARγ/(*R*)-**16**.

Only a few examples of crystalline structures reporting the simultaneous binding of two molecules of a ligand to PPARγ-LBD are known in the literature.[28−30] Among these, the antidiabetic agent **25** (T2384) can adopt two distinct binding

dx.doi.org/10.1021/jm301018z | J. Med. Chem. 2013, 56, 60−72

Table 2. Thermodynamic Parameters Relating to the Formation of the Complexes PPARγ-LBD/Ligand Determined by the ITC Assay

	$K_a \times 10^5$ (M^{-1})	n^a	ΔG (kcal M^{-1})	ΔH (kcal M^{-1})	$-T\Delta S$ (kcal M^{-1})
1	4.59	0.91	−7.72	−8.61	0.89
(*S*)-**16**, site A	3.60	1.09	−7.58	−6.29	−1.29
(*S*)-**16**, reverse titration (A + B)	3.10	0.54	−7.47	−11.26	3.79
(*S*)-**16**, pre-equilibrated with **1** (B)	1.87	0.70	−7.19	−4.15	−3.04
(*R*)-**16**, site B	1.34	0.99	−6.99	−2.37	−4.62
(*R*)-**16**, reverse titration (B + C)	1.30	0.44	−6.97	−6.23	−0.74

[a] *n* = molar binding ratio of the ligand−protein interaction (observed stoichiometry).

modes in the LBD of PPARγ, each of which is able to induce distinct patterns of coregulatory protein interaction with PPARγ in vitro displaying unique receptor functions in cell-based activity assays.[28]

In Figures 6−9 of the Supporting Information the superpositions of (*S*)-**16** with **25**, **26** (HODE-9),[29] and **27** (AF3369)[30] all simultaneously bound with two molecules to the LBD of PPARγ are shown. Although the superpositions are not identical, it can be noted that in all cases one molecule occupies the region in front of the β-sheet whereas the second molecule lies in a region closer to helix 12.

Molecular Modeling. To test whether the ligand binding pocket of PPARγ can host two molecules of (*S*)-**16** simultaneously, we carried out docking calculations on the above-reported two-ligand-bound PPARγ crystal structure. With this purpose, we examined the relative positions of two docked (*S*)-**16** molecules with respect to the bound conformations of (*S*)-**16** in the X-ray crystal structure at site A and site B. The two (*S*)-**16** molecules were sequentially docked through the automated docking software GOLD 5.0.1,[31,32] using the GoldScore-CS docking protocol[33] (see the Experimental Section for details). The first docked (*S*)-**16** conformation was similar to the one seen in site A of the crystal structure (rmsd = 0.7 Å) with the same contact residues. The second (*S*)-**16** molecule was then docked and assumed orientations different from the one seen in the crystal structure at site B (data not shown), indicating the outward movement of the ligand as a consequence of negative cooperativity between two sites. The docking scores of (*S*)-**16** were higher for site A (47.2 kJ/mol) than site B (30.9 kJ/mol), implying that this molecule has extremely low binding affinity toward site B. Together, these results confirm that there is a preference of site A to be the primary site for (*S*)-**16** binding, corroborating the hypothesis that, as observed in ITC experiments, PPARγ can host two molecules of (*S*)-**16** only in presence of a high concentration of this ligand.

To help interpretation of structure−activity relationship (SAR) data and to gain a better understanding of how the described (aryloxy)phenylpropanoic acids might bind to PPARα, we performed docking experiments of the most active **12**, **13**, **15**, and (*S*)-**16** into the ligand binding site of the previously reported cocrystal structure of PPARα bound to the α/γ dual agonist **28** (BMS-631707) (PDB code 2REW).[34] When **12**, **15**, and (*S*)-**16** were docked within the PPARα binding site, about 80% of the conformations generated by GOLD adopted only one highly conserved orientation. Figure 5 depicts the binding mode of the representative compound (*S*)-**16** into the PPARα binding site. Interestingly, the ligands assume a position very similar to that of the cocrystallized **28** and are stabilized by a combination of H-bonds and hydrophobic interactions. The carboxylate group forms the well-recognized H-bonding network with S280 (H3), Y314 (H5), H440 (H11), and Y464 (H12), which is believed to be critical for the functional activity of PPAR ligands. The remaining interactions between ligands and protein are hydrophobic in nature. In particular, the substituted biphenyl moiety lodges into a hydrophobic pocket (pocket I), corresponding to the "biphenyl pocket" in PPARγ, and interacts with F351 and I354 of H7, V444 and I447 of H11, A454 and L456 of the loop 11/12, and F273, C276, and Q277 of H3. Notably, F273 forms a face−edge−face aromatic-stacking interaction with the first aromatic ring of the substituted biphenyl moiety of the ligands. The isopropyl group of (*S*)-**16** establishes hydrophobic interactions with F273, F351, I354, and I447. These results are consistent with the SAR data showing that compounds **12** and **15**, which bear a lipophilic group at the 2′ position of the biphenyl moiety (ethyl and trifluoromethyl, respectively), are highly potent PPARα

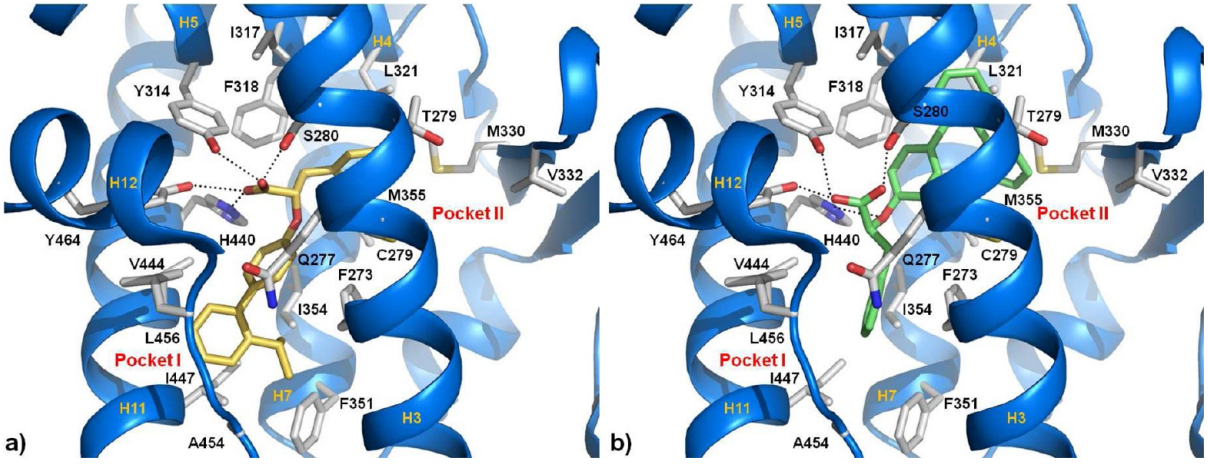

Figure 5. Compounds (*S*)-**16** (a, yellow) and **13** (b, green) docked into the PPARα binding site represented as a blue ribbon model. Only amino acids located within 4 Å of the bound ligand are displayed (white) and labeled. H-bonds discussed in the text are depicted as dashed black lines.

dx.doi.org/10.1021/jm301018z | J. Med. Chem. 2013, 56, 60−72

agonists. In addition, the benzyl ring of the ligands binds in a second hydrophobic pocket (pocket II), making lipophilic interactions with residues C276, T279 of H3, I317, F318, and L321 of H4, M330 of β-sheet, and M355 of H7. It is known that hydrophobic sulfur and especially sulfur−arene interactions are strongly attractive.[35,36] Figure 5 shows that the environment of the benzyl moiety is very rich in S-containing protein side chains (C276, M330, M355), so hydrophobic intermolecular contacts with the ligands are formed, further contributing to the complex stability. Moreover, the stabilization of H11, H3, the loop 11/12, and H12 upon ligand binding could explain the nanomolar activity of **12**, **15**, and (*S*)-**16** and their character of full agonists toward PPARα. Curiously, when compound **13** was docked into the PPARα binding cleft, only 10% of the generated conformations adopted the above-described binding mode, whereas 90% were in a different orientation that positioned both benzyl and substituted biphenyl moieties in a reverse mode within the two above-mentioned hydrophobic pockets. It is likely that the much larger phenyl ring at the 2′ position of the biphenyl moiety does not find sufficient room to be accommodated inside the hydrophobic pocket I, forcing the ligand to adopt a different pose into PPARα. The carboxylate group still engages H-bonds with S280, Y314, and Y464. In addition, an additional H-bond between the phenoxylic oxygen atom of **13** and the H440 $N^{\epsilon}H$ hydrogen is formed. The benzyl substituent occupies, but does not completely fill, the hydrophobic pocket I formed by helices 3, 7, and 11 and the loop 11/12. The remainder of the ligand wraps around helix 3 and buries the phenyl-substituted biphenyl moiety into the lipophilic pocket II formed by helices 3, 4, and 7 and the β sheet.

Effects of (*S*)-16 on the Carnitine Shuttle System. Oxidation of fatty acids in mitochondria coupled to oxidative phosphorylation is the most important pathway for the production of metabolic energy during fasting. This process occurs in the mitochondrial matrix where the enzymes of fatty acid β-oxidation are located. Fatty acyl groups are transported from the cytosol into the mitochondrial matrix by means of the carnitine shuttle system. In the cytosol, fatty acid units are transferred from acyl-CoAs to carnitine by the action of CPT1, which is located on the external surface of the outer mitochondrial membrane;[37,38] the formed acylcarnitines cross the outer membrane, which is permeable to small molecules,[39] and are translocated through the inner mitochondrial membrane by the CAC. CAC is an integral protein that transports acylcarnitine esters (in exchange for free carnitine) into mitochondria where the acyl groups are oxidized. Therefore, the molecular components of the carnitine shuttle system are essential for the mitochondrial oxidation of fatty acids and, hence, for life.[40]

It has been previously demonstrated that the two fibrates Wy 14,643 and **29** (GW7647) increase the CAC transcript level in primary and secondary cell lines, providing, therefore, a novel contribution to the understanding of their hypolipidemic action.[23] On this basis, we decided to test (*S*)-**16** to evaluate the possibility that this fibratelike drug was able, in the same way, to upregulate mitochondrial CAC as well as CPT1 gene expression. The effects of in vitro application of this compound were investigated on HepG2 cells which were incubated for 24 h with a 1 μM concentration of (*S*)-**16**. Wy 14,643 (50 μM) and **29** (1 μM) were used as reference compounds. After incubation, total mRNA was extracted and used to determine CAC and CPT1 transcript levels. As shown in Figures 6A and 7A, (*S*)-**16** caused a CAC and CPT1 mRNA increase of about 1.5- and 2.3-fold in HepG2 cells, respectively. Consistently, Western blotting analysis confirmed markedly increased CAC and CPT1 protein levels (Figures 6B and 7B) in cells treated with (*S*)-**16** as compared to untreated cells. The observed effects of (*S*)-**16** on both CAC and CPT1 gene expression levels turned out to be lower than those obtained with **29** and comparable to those of Wy 14,643. However, the concentration of Wy 14,643 needed to activate both genes is 50-fold higher (50 μM) as compared to that of (*S*)-**16** (1 μM). These results clearly indicate that (*S*)-**16** is a potent upregulator of gene expression of CAC and CPT1, two key proteins of the mitochondrial fatty acid oxidation pathway. Moreover, even though less potent than the selective PPARα ligand **29**, (*S*)-**16** shows a dual full PPARα and partial PPARγ agonist activity that is currently considered as a very attractive option in the treatment of dyslipidemic type 2 diabetes.

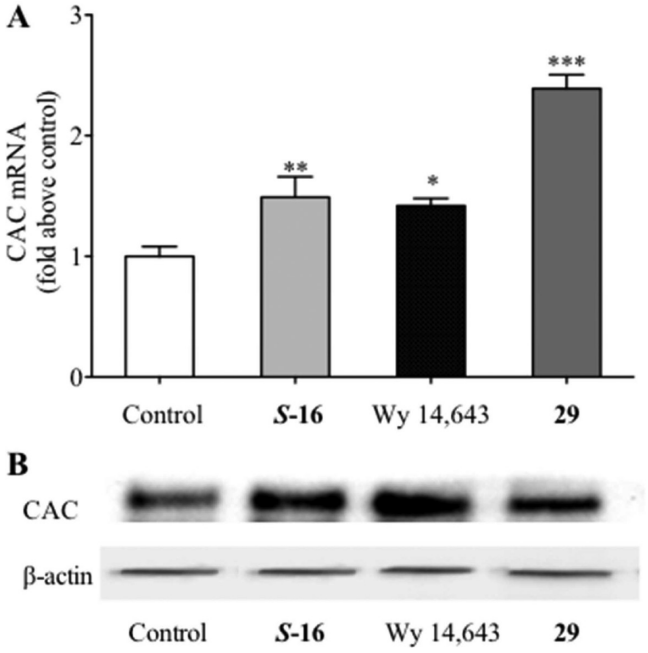

Figure 6. (A) Total RNA extracted from HepG2 cells, treated with or without 1 μM **29**, 50 μM Wy 14,643, or 1 μM (*S*)-**16** for 24 h, was used to quantify CAC mRNA by real-time PCR. (B) CAC and β-actin of HepG2 cells, treated for 48 h as described for (A), were immunodecorated with specific antibodies. In (A) means ± SD of three duplicate independent experiments are shown. In (A), differences between the samples and control (without any addition) were significant (*, $P < 0.05$; **, $P < 0.01$; ***, $P < 0.001$; one-way ANOVA, Bonferroni test).

CONCLUSION

In the present study, we have investigated the effects resulting from the introduction of different substituents into the biphenyl system of compound **1**, previously reported as a PPARα/γ dual agonist. This modification allowed the identification of new ligands with higher potency on PPARα and fine adjusted moderate activity on PPARγ. For the most promising stereoisomer (*S*)-**16**, X-ray and calorimetric studies in PPARγ and docking experiments in both receptor subtypes provided a molecular explanation for its different behavior as a full and partial agonist of PPARα and PPARγ, respectively. Interestingly, it has been observed that PPARγ can host two molecules of (*S*)-**16** in the presence of a high concentration of this ligand,

dx.doi.org/10.1021/jm301018z | J. Med. Chem. 2013, 56, 60−72

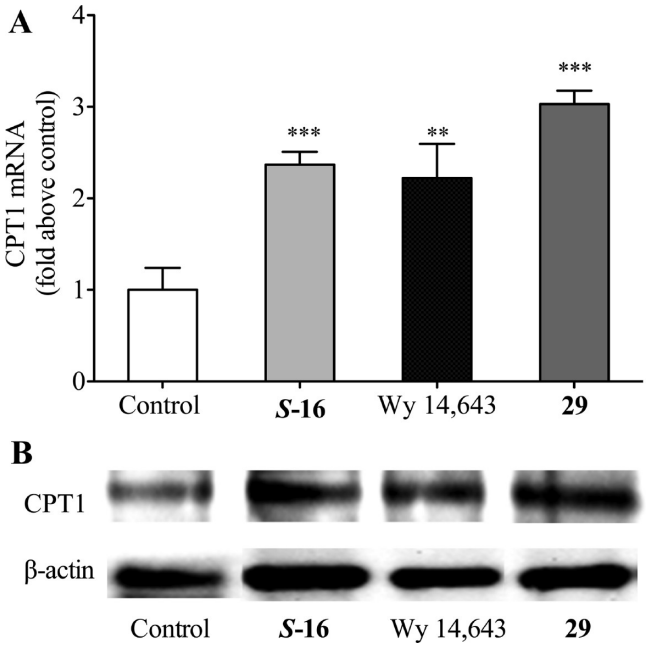

Figure 7. (A) Total RNA extracted from HepG2 cells, incubated with or without 1 μM **29**, 50 μM Wy 14,643, or 1 μM (*S*)-**16** for 24 h, was used to quantify CPT1 mRNA by real-time PCR. (B) CPT1 and β-actin of HepG2 cells, treated for 48 h as described for (A), were immunodecorated with specific antibodies. In (A) means ± SD of three duplicate independent experiments are shown. In (A), differences between the samples and control (without any addition) were significant (**, $P < 0.01$; ***, $P < 0.001$; one-way ANOVA, Bonferroni test).

and its relative affinities for the two sites were determined. Calorimetric data and docking simulations show that at lower ligand concentration the occupation of the only site A is preferred. In addition, the adaptability of PPARγ-LBD has been demonstrated through the rearrangement of several side chains of the internal hydrophobic pocket (F282, R288, E291, etc.), improving the interaction with the ligands. All these features ensure that different ligands, depending on the concentration and the occupied LBD regions, can recruit different classes of coregulators eliciting distinct biological responses. For this reason, even small modifications of the chemical structure of known PPARγ ligands could be able to fine-tune the agonist activity, allowing identification, in a series of strictly related compounds, of the optimal PPARα/PPARγ selectivity ratio.

Moreover, the effects of (*S*)-**16** on the transcription of the mitochondrial CAC and CPT1 genes, two key components of the carnitine shuttle system that is essential for the mitochondrial oxidation of fatty acids, allow the hypothesis of a more beneficial pharmacological profile of this compound in comparison with the less potent PPARα agonist fibrates currently used in therapy. Further studies are in progress to identify the optimal PPARα/γ selectivity ratio in this set of compounds by cofactor recruitment FRET assay for each ligand. In the next step, in vivo experiments will be carried out with the ligands able to recruit cofactors similar to those recruited by selective PPARγ modulators (SPPARγMs) or PPARγ partial agonists currently under clinical investigation to gain insight into the properties and biological action of these molecules, which may represent the potential leads of a new class of drugs with better therapeutic effects in the treatment of dyslipidemic type 2 diabetes.

EXPERIMENTAL SECTION

Chemical Methods. Column chromatography was performed on ICN Silica Gel 60 Å (63–200 μm) as a stationary phase. Melting points were determined in open capillaries on a Gallenkamp electrothermal apparatus and are uncorrected. Mass spectra were recorded on an HP GC/MS 6890-5973 MSD spectrometer, electron impact 70 eV, equipped with an HP chemstation or an Agilent LC/MS 1100 series LC/MSD Trap System VL spectrometer, electrospray ionization (ESI). ^{1}H NMR spectra were recorded in $CDCl_3$ (the use of other solvents is specified) on a Varian-Mercury 300 (300 MHz) spectrometer at room temperature. Chemical shifts are expressed as parts per million (δ). The purity of all tested compounds was >95%, as confirmed by combustion analysis carried out with a Eurovector Euro EA 3000 model analyzer.

Optical rotations were measured with a Perkin-Elmer 341 polarimeter at room temperature (20 °C): concentrations are expressed as grams per 100 mL. The enantiomeric excesses of the final acids were determined by HPLC analysis of acids or their methyl esters, obtained by reaction with an ethereal solution of diazomethane, on a Chiralcel OD or AD column (4.6 mm i.d. × 250 mm, Daicel Chemical Industries, Ltd., Tokyo, Japan). Analytical liquid chromatography was performed on a PE chromatograph equipped with a Rheodyne 7725i model injector, a 785A model UV/vis detector, a series 200 model pump, and an NCI 900 model interface. Chemicals were from Aldrich (Milan, Italy), AlfaAesar (Karlsruhe, Germany), or Acros (Milan, Italy) and were used without any further purification.

Preparation of Ethyl 2-(Aryloxy)-3-phenylpropanoates 20a–g: General Procedure. To an ice-bath-cooled suspension of PPh_3–DVB[22] (2% DVB, 3 mmol g^{-1}, 13.8 mmol) in anhydrous toluene (35 mL) was added dropwise a solution of diisopropyl azodicarboxylate (DIAD; 13.5 mmol) in anhydrous toluene (35 mL). The resulting mixture was stirred for 0.5 h. A solution of the suitable *R* or *S* enantiomer or racemic ethyl phenyllactate (11 mmol) in anhydrous toluene (50 mL) and suitable 4-bromophenol (10 mmol) was added at rt. The reaction mixture was stirred overnight at rt under a N_2 atmosphere. The solid was filtered off, and the filtrate was evaporated to dryness. The residue was chromatographed on a silica gel column (petroleum ether/ethyl acetate, 9:1 or 8:2, as eluent), affording the desired compounds as pale yellow oils in 54–82% yields.

Preparation of Ethyl 2-(Biaryl-4-yloxy)-3-phenylpropanoates 21a–r: General Procedure. The suitable arylboronic acid (3.64 mmol) and Cs_2CO_3 (2.73 mmol) were added, under a N_2 atmosphere, to a stirred solution of the corresponding compounds **20a–g** synthesized as above (1.82 mmol) in anhydrous toluene (35 mL); after 0.5 h, $Pd(PPh_3)_4$ (0.11 mmol) or $Pd(PPh_3)_4$–DVB (2% DVB, 0.5 mmol g^{-1}, 0.055 mmol) was added. The reaction mixture was stirred overnight at 95 °C and then quenched with 1 N HCl (7.5 mL) and ethyl acetate (7.5 mL). The suspension was filtered through a Celite pad to remove the catalyst, and the filtrate was washed with $NaHCO_3$ saturated solution and brine. After the filtrate was dried over Na_2SO_4, the solvent was evaporated to dryness to give a dark oily residue which was chromatographed on a silica gel column (petroleum ether/ethyl acetate, 98:2 or 95:5, as eluent), affording the desired compounds as colorless or yellow oils in 25–95% yields.

Synthesis of Ethyl 2-[(2′-Formylbiphenyl-4-yl)oxy]-3-phenylpropanoate (22). In a suitable vessel, a mixture of **20c** (2.87 mmol), 2-formylbenzeneboronic acid (4.29 mmol), and Cs_2CO_3 (5.73 mmol) was dissolved in 45 mL of THF. After 20 min $Pd(PPh_3)_4$ (0.17 mmol) was added, and the resulting suspension was vigorously stirred in a microwave reactor (1 h, 100 °C, 150 W). The resulting crude was filtered through a Celite pad to remove the catalyst, and the filtrate was washed with $NaHCO_3$ saturated solution and brine. After the filtrate was dried over Na_2SO_4, the solvent was evaporated to dryness to give a dark oily residue which was chromatographed on a silica gel column (*n*-hexane/ethyl acetate, 98:2, as eluent), affording the desired compound as a yellow oil.

Synthesis of Ethyl 2-[(2′-Substituted biphenyl-4-yl)oxy]-3-phenylpropanoates 23a–c: General Procedure. A solution of **22** (2.5 mmol) in anhydrous CH_3CN (20 mL) was carefully added, under a N_2 atmosphere and during 0.5 h, to a stirred solution of the

dx.doi.org/10.1021/jm301018z | J. Med. Chem. 2013, 56, 60–72

appropriate alkyl- or (arylalkyl)triphenylphosphonium bromide (5 mmol) in anhydrous CH_3CN (15 mL). After 0.5 h a solution of DBU (5 mmol) in dry CH_3CN (15 mL) was added to the mixture. The reaction mixture was stirred and heated under reflux for 24 h, the solvent was removed under reduced pressure, and the residue was dissolved in ethyl acetate. The organic phase was washed with NH_4Cl saturated solution and twice with brine, then dried over Na_2SO_4, and filtered. The solvent was evaporated to dryness, affording crude oils which were chromatographed on a silica gel column (petroleum ether/ethyl acetate, 95:5, as eluent) to obtain colorless oils in 17−54% yields.

Synthesis of Ethyl 2-[(2′-Substituted biphenyl-4-yl)oxy]-3-phenylpropanoates 24a−c: General Procedure. The oily mixtures of *cis* and *trans* isomers **23a−c** (1 mmol) were dissolved in absolute EtOH (90 mL) and stirred at rt under a H_2 atmosphere (10−15 atm) in the presence of the Wilkinson catalyst or 10% Pd/C (0.05 mmol). After 24−48 h the suspension was filtered through a Celite pad to remove the catalyst, and the filtrate was concentrated under reduced pressure to give dark solids which were chromatographed on a silica gel column (Et_2O/CH_2Cl_2, 90:10 or 80:20, or petroleum ether/ethyl acetate, 80:20, as eluent), affording the title compounds as colorless oils in 84−93% yields.

Preparation of the Final Acids 2−19: General Procedure. To a stirred solution of the corresponding ethyl ester (1 mmol) in THF (10 mL) was added 1 or 2 N NaOH (10 mL). The reaction mixture was stirred for 4−10 h. THF was evaporated in vacuo, and the aqueous phase was acidified with 2 N HCl and extracted with Et_2O. The combined organic layers were washed twice with brine, dried over Na_2SO_4, and evaporated to dryness, affording the title acids in quantitative yields as white solids or colorless oils. The oily acids were dissolved in 96% EtOH (10 mL) and added to a solution of $NaHCO_3$ (1 equiv) in H_2O (1 mL). The reaction mixture was stirred for 2 h, and then the solvent was evaporated to dryness, affording the corresponding sodium salts in quantitative yields as white solids which were washed or crystallized from the suitable solvents.

Biological Methods. Reference compounds, the medium, and other cell culture reagents were purchased from Sigma-Aldrich (Milan, Italy).

Plasmids. The expression vectors expressing the chimeric receptor containing the yeast Gal4-DNA binding domain fused to the human PPARα- or PPARγ-LBD and the reporter plasmid for these Gal4 chimeric receptors (pGal5TKpGL3) containing five repeats of the Gal4 response elements upstream of a minimal thymidine kinase promoter that is adjacent to the luciferase gene were described previously.[41]

Cell Culture and Transfections. Human hepatoblastoma cell line HepG2 (Interlab Cell Line Collection, Genoa, Italy) was cultured in minimum essential medium (MEM) containing 10% heat-inactivated fetal bovine serum, 100 U of penicillin G mL^{-1}, and 100 μg of streptomycin sulfate mL^{-1} at 37 °C in a humidified atmosphere of 5% CO_2. For transactivation assays, 10^5 cells per well were seeded in a 24-well plate and transfections were performed after 24 h with CAPHOS, a calcium phosphate method, according to the manufacturer's guidelines. Cells were transfected with expression plasmids encoding the fusion protein Gal4−PPARα-LBD or Gal4−PPARγ-LBD (30 ng), pGal5TKpGL3 (100 ng), and pCMVβgal (250 ng). Four hours after transfection, cells were treated for 20 h with the indicated ligands in triplicate. Luciferase activity in cell extracts was then determined by a luminometer (VICTOR^3 V Multilabel Plate Reader, PerkinElmer). β-Galactosidase activity was determined using ortho-nitro-phenyl-β-D-galactopyranoside as described previously.[42] All transfection experiments were repeated at least twice.

Real-Time PCR. HepG2 cells were incubated for 24 h with Wy 14,643 (50 μM), **29** (1 μM), and (*S*)-**16** (1 μM), starting 24 h after having been depleted of serum. Total RNA was extracted from 1×10^6 cells, and reverse transcription was performed as reported.[43] Real-time PCR was carried out as described previously.[44] Assays-on-demand for human CPT1, CAC, and human actin (catalog nos. Hs00912671_m1, Hs01088810_g1, and Hs00357333_g1, respectively) were purchased from Applied Biosystems. All transcript levels were normalized against the β-actin expression levels.

Western Blot Analysis. HepG2 cells were incubated for 48 h with Wy 14,643 (50 μM), **29** (1 μM), and (*S*)-**16** (1 μM), starting 24 h after having been depleted of serum. Proteins were electroblotted onto nitrocellulose membranes (Bio-Rad) and subsequently treated with anti-CPT1 (ARP44796_P050, Aviva Systems Biology), anti-CAC,[23] and anti-β-actin (sc-58619, Santa Cruz) antibodies. The immunoreaction was detected by the ECL plus system (Amersham).

Protein Expression, Purification, and Crystallization. The LBD of PPARγ was expressed as an N-terminal His-tagged protein using a peT28 vector and purified onto a Ni^{2+}−nitriloacetic acid column (GE Healthcare) as previously described.[45] Crystals of apo-PPARγ were obtained by the vapor diffusion method at 18 °C using a sitting drop made by mixing 2 μL of protein solution (12 mg/mL, in 20 mM Tris and 1 mM TCEP, pH 8.0) with 2 μL of reservoir solution (0.8 M sodium citrate and 0.15 M Tris, pH 8.0). The crystals were soaked for one week in a storage solution (1.2 M sodium citrate and 0.15 M Tris, pH 8.0) containing the ligand (0.5 mM). The ligand dissolved in DMSO was diluted in the storage solution so that the final concentration of DMSO was 0.5%. The storage solution with glycerol [20% (v/v)] was used as a cryoprotectant. Crystals belong to the space group *C*121 with cell parameters shown in Table 1 of the Supporting Information.

Structure Determination. X-ray data were collected at 100 K under a nitrogen stream using synchrotron radiation (beamline ID 23-2 at ESRF, Grenoble, France). The diffracted intensities were processed using the programs MOSFLM and SCALA.[46] Structure solution was performed with AMoRe,[47] using the coordinates of PPARγ/**1** (PDB code 3B3K) as the starting model. The coordinates were then refined with CNS.[48] All data between 8 and 2.5 Å were included. The statistics of crystallographic data and refinement are summarized in Table 1 of the Supporting Information. The coordinates of PPARγ/(*S*)-**16** and PPARγ/(*R*)-**16** have been deposited in the Brookhaven Protein Data Bank (PDB) with the codes 4E4K and 4E4Q, respectively.

Isothermal Titration Calorimetry. ITC experiments were performed at 25 °C using a MicroCal ITC_{200} microcalorimeter (MicroCal Inc., Northampton, MA). PPARγ was extensively dialyzed against the buffer Hepes (20 mM, pH 8.0), TCEP (1 mM), with Amicon Ultra filters, and the final exchange buffer was then used to dilute the ligand stock solutions (50 mM in DMSO). DMSO was added to the protein solution at the same percentage of the ligand solution (below 1%). Samples were centrifuged before the experiments to eliminate possible aggregates. Protein and ligand solutions were degassed before use. The protein solution (40 μM) was placed in the sample cell, and the ligand solution (400 μM) was loaded into the syringe injector. In the reverse titration the protein solution (400 μM) was injected into the cell containing the ligand (40 μM). The titrations involved 19 injections of 2 μL at 180 s intervals. The syringe stirring speed was set at 1000 rpm. Reference titrations of ligands into buffer were used to correct for heats of dilution. The thermodynamic data were processed with Origin 7.0 software provided by MicroCal. The ΔH values were measured for each titration, and fitting the binding isotherms with a one-site binding model yielded the values of the association constant (K_a). From the Gibbs−Helmholtz equation is also calculated the change of entropy (ΔS). The inflection point in the calorimetric isotherm gives the stoichiometry value *n*, indicating the ligand/protein ratio of the binding. To correct for any discrepancies in the baseline outlined by the software, a manual adjustment was performed. In one experiment the protein was preliminarily equilibrated with the ligand for 3 h.

Computational Chemistry. Molecular modeling and graphics manipulations were performed using the molecular operating environment (MOE)[49] and UCSF-Chimera software packages,[50] running on an E4 Computer Engineering E1080 workstation provided with an Intel Core i7-930 Quad-Core processor. GOLD 5.0.1[31] was used for all docking calculations. Figures were generated using Pymol 1.0.[51]

Ligand and Protein Setup. The core structures of compounds **12**, **13**, **15**, and (*S*)-**16** were constructed using standard bond lengths and bond angles of the MOE fragment library. The carboxylate group

dx.doi.org/10.1021/jm301018z | J. Med. Chem. 2013, 56, 60−72

was taken as dissociated. Geometry optimizations were accomplished with the MMFF94X force field, available within MOE. The coordinates of PPARγ/(*S*)-**16** (PDB code 4E4K) and PPARα/**28** (PDB code 2REW),[34] recovered from the Brookhaven Protein Database,[52] were used in the docking experiments. Bound ligands and water molecules were removed. A correct atom assignment for Asn, Gln, and His residues was done, and hydrogen atoms were added using standard MOE geometries. Partial atomic charges were computed by MOE using the AMBER99 force field. All heavy atoms were then fixed, and hydrogen atoms were minimized using the AMBER99 force field and a constant dielectric of 1, terminating at a gradient of 0.001 kcal mol^{-1} $Å^{-1}$.

Docking Simulations. Docking of (*S*)-**16** to PPARγ and **12**, **13**, **15**, and (*S*)-**16** to PPARα was performed with the GOLD program, which uses a genetic algorithm for determining the docking modes of ligands and proteins. In the present study, GOLD was allowed to calculate interaction energies within a sphere of a 7 Å radius centered around the two bound (*S*)-**16** molecules for site A and site B of PPARγ and a 13 Å sphere radius centered on the cocrystallized ligand **28** of PPARα. The Goldscore-CS docking protocol[33] was adopted in this study. In this protocol, the poses obtained with the original GoldScore function are rescored and reranked with the GOLD implementation of the ChemScore function.[33,53] To perform a thorough and unbiased search of the conformation space, each docking run was allowed to produce 200 poses without the option of early termination, using standard default settings. The docking procedure employed for initial exploration of multiple ligand binding to PPARγ was analogous to one that was explored by a number of groups whose aim was to probe the structural basis of heterotropic/homotropic activation or inhibition.[54,55] In this approach, two ligands were docked in a sequential fashion. The first ligand was docked using a pre-evaluated interaction grid based on interactions with atoms in the protein alone. The second ligand was then docked employing an interaction grid including interactions with the protein and bound configurations of the first ligand. In this way, the energy landscape for binding of the second ligand includes interactions with the first ligand. It is plausible that the binding of multiple ligands to PPARγ involves such a sequential process. Cobound configurations of two (*S*)-**16** molecules were searched by first determining the unique sets of clustered configurations of one of the two ligands, using an rmsd criterion of 1.5 Å, followed by docking the second ligand to a representative structure for clusters of the first docked ligand.

■ ASSOCIATED CONTENT

Supporting Information

Physicochemical properties and spectroscopic data for intermediates and final compounds, statistics of crystallographic data and refinement, superposition of (*R*)-**16** and Mol B of (*S*)-**16** into the LBD of PPARγ, titration curve of PPARγ with **1** and (*R*)-**16**, reverse titration curve of (*R*)-**16** with PPARγ, and superposition of (*S*)-**16** and PPARγ partial agonists **25**, **26**, and **27** into the PPARγ-LBD. This material is available free of charge via the Internet at http://pubs.acs.org.

Accession Codes

PDB IDs 4E4K, 4E4Q, 3B3K, and 2REW.

■ AUTHOR INFORMATION

Corresponding Author

*Phone: +39 080-5442778. Fax: +39 080-5442231. E-mail: fulvio.loiodice@uniba.it.

Notes

The authors declare no competing financial interest.

■ ACKNOWLEDGMENTS

This work was accomplished thanks to the financial support of the Università degli Studi di Bari "Aldo Moro" (Research Fund 2010).

■ ABBREVIATIONS USED

PPAR, peroxisome proliferator-activated receptor; LBD, ligand binding domain; TZDs, thiazolidinediones; CAC, carnitine/acylcarnitine carrier; CPT1, carnitine-palmitoyl-transferase 1; ITC, isothermal titration calorimetry

■ REFERENCES

(1) Kliewer, S. A.; Sundseth, S. S.; Jones, S. A.; Brown, P. J.; Wisely, G. B.; Koble, C. S.; Devchand, P.; Wahli, W.; Willson, T. M.; Lenhard, J. M.; Lehmann, J. M. Fatty acids and eicosanoids regulate gene expression through direct interactions with peroxisome proliferator-activated receptors α and γ. *Proc. Natl. Acad. Sci. U.S.A.* **1997**, *94*, 4318−4323.

(2) Berger, J. P.; Akiyama, T. E.; Meinke, P. T. PPARs: therapeutic targets for metabolic disease. *Trends Pharmacol. Sci.* **2005**, *26*, 244−251.

(3) Nagy, L.; Schwabe, J. W. Mechanism of the nuclear receptor molecular switch. *Trends Biochem. Sci.* **2004**, *29*, 317−324.

(4) Nettles, K. W.; Greene, G. L. Ligand control of coregulator recruitment to nuclear receptors. *Annu. Rev. Physiol.* **2005**, *67*, 309−333.

(5) Renaud, J. P.; Moras, D. Structural studies on nuclear receptors. *Cell. Mol. Life Sci.* **2000**, *57*, 1748−1769.

(6) Desvergne, B.; Wahli, W. Peroxisome proliferator-activated receptors: nuclear control of metabolism. *Endocr. Rev.* **1999**, *20*, 649−688.

(7) Elisaf, M. Effects of fibrates on serum metabolic parameters. *Curr. Med. Res. Opin.* **2002**, *18*, 269−276.

(8) Staels, B.; Dallongeville, J.; Auwerx, J.; Schoonjans, K.; Leitersdorf, E.; Fruchart, J.-C. Mechanism of action of fibrates on lipid and lipoprotein metabolism. *Circulation* **1998**, *98*, 2088−2093.

(9) Campbell, I. W. The clinical significance of PPAR gamma agonism. *Curr. Mol. Med.* **2005**, *5*, 349−363.

(10) Reifel Miller, A. Today's challenges and tomorrow's opportunities: ligands to peroxisome proliferator-activated receptors as therapies for type 2 diabetes and metabolic syndrome. *Drug Dev. Res.* **2006**, *67*, 574−578.

(11) Henke, B. R. Peroxisome proliferator-activated receptor α/γ dual agonists for the treatment of type 2 diabetes. *J. Med. Chem.* **2004**, *47*, 4118−4127.

(12) Lohray, B. B.; Lohray, V. B.; Bajji, A. C.; Kalchar, S.; Poondra, R. R.; Padakanti, S.; Chakrabarti, R.; Vikramadithyan, R. K.; Misra, P.; Juluri, S.; Mamidi, N. V.; Rajagopalan, R. (−)3-[4-[2-(Phenoxazin-10-yl)ethoxy]phenyl]-2-ethoxypropanoic acid [(−)DRF 2725]: a dual PPAR agonist with potent antihyperglycemic and lipid modulating activity. *J. Med. Chem.* **2001**, *44*, 2675−2678.

(13) Sauerberg, P.; Pettersson, I.; Jeppesen, L.; Bury, P. S.; Mogensen, J. P.; Wassermann, K.; Brand, C. L.; Sturis, J.; Woldike, H. F.; Fleckner, J.; Andersen, A. S.; Mortensen, S. B.; Svensson, L. A.; Rasmussen, H. B.; Lehmann, S. V.; Polivka, Z.; Sindelar, K.; Panajotova, V.; Ynddal, L.; Wulff, E. M. Novel tricyclic-α-alkyloxyphenylpropionic acids: dual PPARα/γ agonists with hypolipidemic and antidiabetic activity. *J. Med. Chem.* **2002**, *45*, 789−804.

(14) Ebdrup, S.; Pettersson, I.; Rasmussen, H. B.; Deussen, H. J.; Frost Jensen, A.; Mortensen, S. B.; Fleckner, J.; Pridal, L.; Nygaard, L.; Sauerberg, P. Synthesis and biological and structural characterization of the dual-acting peroxisome proliferator-activated receptor α/γ agonist ragaglitazar. *J. Med. Chem.* **2003**, *46*, 1306−1317.

(15) Devasthale, P. V.; Chen, S.; Jeon, Y.; Qu, F.; Shao, C.; Wang, W.; Zhang, H.; Cap, M.; Farrelly, D.; Golla, R.; Grover, G.; Harrity, T.; Ma, Z.; Moore, L.; Ren, J.; Seethala, R.; Cheng, L.; Sleph, P.; Sun, W.; Tieman, A.; Wetterau, J. R.; Doweyko, A.; Chandrasena, G.; Chang, S.

Y.; Humphreys, W. G.; Sasseville, V. G.; Biller, S. A.; Ryono, D. E.; Selan, F.; Hariharan, N.; Cheng, P. T. Design and synthesis of *N*-[(4-methoxyphenoxy)carbonyl]-*N*-[[4-[2-(5-methyl-2-phenyl-4-oxazolyl)-ethoxy]phenyl]methyl]glycine [Muraglitazar/BMS-298585], a novel peroxisome proliferator-activated receptor α/γ dual agonist with efficacious glucose and lipid-lowering activities. *J. Med. Chem.* **2005**, *48*, 2248−2250.

(16) Koyama, H.; Miller, D. J.; Boueres, J. K.; Desai, R. C.; Jones, A. B.; Berger, J. P.; MacNaul, K. L.; Kelly, L. J.; Doebber, T. W.; Wu, M. S.; Zhou, G.; Wang, P. R.; Ippolito, M. C.; Chao, Y. S.; Agrawal, A. K.; Franklin, R.; Heck, J. V.; Wright, S. D.; Moller, D. E.; Sahoo, S. P. (2*R*)-2-Ethylchromane-2-carboxylic acids: discovery of novel PPARα/γ dual agonists as antihyperglycemic and hypolipidemic agents. *J. Med. Chem.* **2004**, *47*, 3255−3263.

(17) Shi, G. Q.; Dropinski, J. F.; McKeever, B. M.; Xu, S.; Becker, J. W.; Berger, J. P.; MacNaul, K. L.; Elbrecht, A.; Zhou, G.; Doebber, T. W.; Wang, P.; Chao, Y. S.; Forrest, M.; Heck, J. V.; Moller, D. E.; Jones, A. B. Design and synthesis of α-aryloxyphenylacetic acid derivatives: a novel class of PPARα/γ dual agonists with potent antihyperglycemic and lipid modulating activity. *J. Med. Chem.* **2005**, *48*, 4457−4468.

(18) Ljung, B.; Bamberg, K.; Dahllof, B.; Kjellstedt, A.; Oakes, N. D.; Ostling, J.; Svensson, L.; Camejo, G. AZ 242, a novel PPARα/γ agonist with beneficial effects on insulin resistance and carbohydrate and lipid metabolism in ob/ob mice and obese Zucker rats. *J. Lipid Res.* **2002**, *43*, 1855−1863.

(19) Grey, A. Skeletal consequences of thiazolidinedione therapy. *Osteoporosis Int.* **2008**, *19*, 129−137.

(20) Rubenstrunk, A.; Hanf, R.; Hum, D. W.; Fruchart, J.-C.; Staels, B. Safety issues and prospects for future generations of PPAR modulators. *Biochim. Biophys. Acta* **2007**, *1771*, 1065−1081.

(21) Shearer, B. G.; Billin, A. N. The next generation of PPAR drugs: do we have the tools to find them? *Biochim. Biophys. Acta* **2007**, *1771*, 1082−1093.

(22) Montanari, R.; Saccoccia, F.; Scotti, E.; Crestani, M.; Godio, C.; Gilardi, F.; Loiodice, F.; Fracchiolla, G.; Laghezza, A.; Tortorella, P.; Lavecchia, A.; Novellino, E.; Mazza, F.; Aschi, M.; Pochetti, G. Crystal structure of the peroxisome proliferator-activated receptor γ (PPARγ) ligand binding domain complexed with a novel partial agonist: a new region of the hydrophobic pocket could be exploited for drug design. *J. Med. Chem.* **2008**, *51*, 7768−7776.

(23) Iacobazzi, V.; Convertini, P.; Infantino, V.; Scarcia, P.; Todisco, S.; Palmieri, F. Statins, fibrates and retinoic acid upregulate mitochondrial acylcarnitine carrier gene expression. *Biochem. Biophys. Res. Commun.* **2009**, *388*, 643−647.

(24) Indiveri, C.; Iacobazzi, V.; Tonazzi, A.; Giangregorio, N.; Infantino, V.; Convertini, P.; Console, L.; Palmieri, F. The mitochondrial carnitine/acylcarnitine carrier: function, structure and physiopathology. *Mol. Aspects Med.* **2011**, *32*, 223−233.

(25) Gutgesell, A.; Wen, G.; König, B.; Koch, A.; Spielmann, J.; Stangl, G. I.; Eder, K.; Ringseis, R. Mouse carnitine-acylcarnitine translocase (CACT) is transcriptionally regulated by PPARα and PPARδ in liver cells. *Biochim. Biophys. Acta, Gen. Subj.* **2009**, *1790*, 1206−16.

(26) Pinelli, A.; Godio, C.; Laghezza, A.; Mitro, N.; Fracchiolla, G.; Tortorella, V.; Lavecchia, A.; Novellino, E.; Fruchart, J. C.; Staels, B.; Crestani, M.; Loiodice, F. Synthesis, biological evaluation, and molecular modeling investigation of new chiral fibrates with PPARα and PPARγ agonist activity. *J. Med. Chem.* **2005**, *48*, 5509−5519.

(27) Bruning, J. B.; Chalmers, M. J.; Prasad, S.; Busby, S. A.; Kamenecka, T. M.; He, Y.; Nettles, K. W.; Griffin, P. R. Partial agonists activate PPARγ using a helix 12 independent mechanism. *J. Med. Chem.* **2007**, *15*, 1258−1271.

(28) Li, Y.; Wang, Z.; Furukawa, N.; Escaron, P.; Weiszmann, J.; Lee, G.; Lindstrom, M.; Liu, J.; Liu, X.; Xu, H.; Plotnikova, O.; Prasad, V.; Walker, N.; Learned, R. M.; Chen, J. L. T2384, a novel antidiabetic agent with unique peroxisome proliferator-activated receptor γ binding properties. *J. Biol. Chem.* **2008**, *283*, 9168−9176.

(29) Itoh, T.; Fairall, L.; Amin, K.; Inaba, Y.; Szanto, A.; Balint, B. L.; Nagy, L.; Yamamoto, K.; Schwabe, J. W. R. Structural basis for the activation of PPARγ by oxidized fatty acids. *Nat. Struct. Mol. Biol.* **2008**, *15*, 924−931.

(30) Communication to Worldpharma 2010 (16th IUPHAR World Congress of Basis and Clinical Pharmacology, Copenhagen, Denmark, July 17−23, 2010; Paper 2908, p 434.

(31) *GOLD*, version 5.0.1; CCDC Software Ltd.: Cambridge, U.K., 2008.

(32) Jones, G.; Willett, P.; Glen, R. C.; Leach, A. R.; Taylor, R. Development and validation of a genetic algorithm for flexible docking. *J. Mol. Biol.* **1997**, *267*, 727−748.

(33) Verdonk, M. L.; Cole, J. C.; Hartshorn, M. J.; Murray, C. W.; Taylor, R. D. Improved protein-ligand docking using GOLD. *Proteins: Struct., Funct., Genet.* **2003**, *52*, 609−623.

(34) Wang, W.; Devasthale, P.; Farrelly, D.; Gu, L.; Harrity, T.; Cap, M.; Chu, C.; Kunselman, L.; Morgan, N.; Ponticiello, R.; Zebo, R.; Zhang, L.; Locke, K.; Lippy, J.; O'Malley, K.; Hosagrahara, V.; Zhang, L.; Kadiyala, P.; Chang, C.; Muckelbauer, J.; Doweyko, A. M.; Zahler, R.; Ryono, D.; Hariharan, N.; Cheng, P. T. Discovery of azetidinone acids as conformationally-constrained dual PPARα/γ agonists. *Bioorg. Med. Chem. Lett.* **2008**, *18*, 1939−1944.

(35) Meyer, E. A.; Castellano, R. K.; Diederich, F. Interactions with aromatic rings in chemical and biological recognition. *Angew. Chem., Int. Ed.* **2003**, *42*, 1210−1250.

(36) Kawatkar, S. P.; Kuntz, D. A.; Woods, R. J.; Rose, D. R.; Boons, G. J. Structural basis of the inhibition of Golgi α-mannosidase II by mannostatin A and the role of the thiomethyl moiety in ligand−protein interactions. *J. Am. Chem. Soc.* **2006**, *128*, 8310−8319.

(37) Lee, K.; Kerner, J.; Hoppel, C. L. Mitochondrial carnitine palmitoyltransferase 1a (CPT1a) is part of an outer membrane fatty acid transfer complex. *J. Biol. Chem.* **2011**, *286*, 25655−25662.

(38) Rufer, A. C.; Thoma, R.; Hennig, M. Structural insight into function and regulation of carnitine palmitoyltransferase. *Cell. Mol. Life Sci.* **2009**, *66*, 2489−2501.

(39) Zeth, K.; Thein, M. Porins in prokaryotes and eukaryotes: common themes and variations. *Biochem. J.* **2010**, *431*, 13−22.

(40) Ramsay, R. R.; Gandour, R. D.; van der Leij, F. R. Molecular enzymology of carnitine transfer and transport. *Biochim. Biophys. Acta* **2001**, *1546*, 21−43.

(41) Raspe, E.; Madsen, L.; Lefebvre, A. M.; Leitersdorf, I.; Gelman, L.; Peinado-Onsurbe, J.; Dallongeville, J.; Fruchart, J.-C.; Berge, R.; Staels, B. Modulation of rat liver apolipoprotein gene expression and serum lipid levels by tetradecylthioacetic acid (TTA) via PPARα activation. *J. Lipid Res.* **1999**, *40*, 2099−2110.

(42) Hollon, T.; Yoshimura, F. K. Variation in enzymatic transient gene expression assays. *Anal. Biochem.* **1989**, *182*, 411−418.

(43) Iacobazzi, V.; Infantino, V.; Convertini, P.; Vozza, A.; Agrimi, G.; Palmieri, F. Transcription of the mitochondrial citrate carrier gene: identification of a silencer and its binding protein ZNF224. *Biochem. Biophys. Res. Commun.* **2009**, *386*, 186−191.

(44) Convertini, P.; Infantino, V.; Bisaccia, F.; Palmieri, F.; Iacobazzi, V. Role of FOXA and Sp1 in mitochondrial acylcarnitine carrier gene expression in different cell lines. *Biochem. Biophys. Res. Commun.* **2011**, *404*, 376−381.

(45) Pochetti, G.; Godio, C.; Mitro, N.; Caruso, D.; Galmozzi, A.; Scurati, S.; Loiodice, F.; Fracchiolla, G.; Tortorella, P.; Laghezza, A.; Lavecchia, A.; Novellino, E.; Mazza, F.; Crestani, M. Insights into the mechanism of partial agonism: crystal structures of the peroxisome proliferator-activated receptor γ ligand-binding domain in the complex with two enantiomeric ligands. *J. Biol. Chem.* **2007**, *282*, 17314−17324.

(46) Leslie, A. G. W. Recent changes to the MOSFLM package for processing film and image plate data. *Jt. CCP4 ESF-EACMB Newsl. Protein Crystallogr.* **1992**, *26*, 27−33.

(47) Navaza, J. AMoRe: an automated package for molecular replacement. *Acta Crystallogr., Sect. A* **1994**, *50*, 157−163.

(48) Brunger, A. T.; Adams, P. D.; Clore, G. M.; DeLano, W. L.; Gros, P.; Grosse-Kunstleve, R. W.; Jiang, J. S.; Kuszewski, J.; Nilges, M.; Pannu, N. S.; Read, R. J.; Rice, L. M.; Simonson, T.; Warren, G. L.

Crystallography NMR system: a new software suite for macromolecular structure determination. *Acta Crystallogr., Sect. D* **1998**, *54*, 905−921.
(49) *Molecular Operating Environment (MOE)*, version 2010.10; Chemical Computing Group, Inc.: Montreal, Canada, 2010; www.chemcomp.com (accessed February 15, 2012).
(50) Huang, C. C.; Couch, G. S.; Pettersen, E. F.; Ferrin, T. E. Chimera: an extensible molecular modeling application constructed using standard components. *Pac. Symp. Biocomput.* **1996**, *1*, 724. Also see the Chimera Home Page. http://www.cgl.ucsf.edu/chimera (accessed February 10, 2012).
(51) DeLano, W. L. *The PyMOL Molecular Graphics System*; DeLano Scientific LLC: San Carlos, CA; http://www.pymol.org/ (accessed April 20, 2012).
(52) Bernstein, F. C.; Koetzle, T. F.; Williams, G. J. B.; Meyer, E. F., Jr.; Brice, M. D.; Rodgers, J. R.; Kennard, O.; Shimanouchi, T.; Tasumi, T. The Protein Data Bank: a computer based archival file for macromolecular structures. *J. Mol. Biol.* **1977**, *112*, 535−542.
(53) Eldridge, M. D.; Murray, C. W.; Auton, T. R.; Paolini, G. V.; Mee, R. P. Empirical scoring functions: I. The development of a fast empirical scoring function to estimate the binding affinity of ligands in receptor complexes. *J. Comput.-Aided Mol. Des.* **1997**, *11*, 425−445.
(54) Muralidhara, B. K.; Negi, S. S.; Halpert, J. R. Dissecting the thermodynamics and cooperativity of ligand binding in cytochrome P450eryF. *J. Am. Chem. Soc.* **2007**, *129*, 2015−2024.
(55) Locuson, C. W.; Gannett, P. M.; Ayscue, R.; Tracy, T. S. Use of simple docking methods to screen a virtual library for heteroactivators of cytochrome P450 2C9. *J. Med. Chem.* **2007**, *50*, 1158−1165.